Frankel equation for turbulent flames in the presence of a hydrodynamic instability

Bruno Denet
Institut de Recherche sur les Phénomènes Hors Equilibre, Combustion Université de Provence, Centre de Saint Jérôme, UMR 138 (S 252), 13397 Marseille Cedex 20, France
(Received 23 December 1996)

An extension of the Frankel equation, coupled to a treatment of reconnections, is used to describe numerically turbulent flames submitted to the hydrodynamic Darrieus-Landau instability. The role played by this instability on the fractal properties of the front is evaluated. [S1063-651X(97)03506-X]

PACS number(s): 47.70.Fw, 82.40.Py

It has been customary to describe turbulent premixed flames as interfaces propagating normally with a given laminar velocity, and submitted to an imposed turbulent flow field [1]. However, it is well known that there is a retroaction of the flame front, which induces a new velocity field, which in turn will also affect the flame wrinkling.

In the case of laminar flames, this retroaction effect leads to the hydrodynamic Darrieus-Landau instability. A nonlinear equation, the Michelson-Sivashinsky equation [2], has been introduced to describe this instability in the limit where the burnt gases are irrotational and where the flame is close to a plane flame. Despite these simplifying hypotheses, this equation had a lot of success in describing correctly most of the nonlinear features observed in laminar flames [3–6]. Extensions of this equation have also been successful in describing spherically expanding flames [7,8]. This Michelson-Sivashinsky equation has been generalized to obtain a coordinate-free equation describing a closed front, the Frankel equation [9] (an alternative way to incorporate heat release into a lagrangian method has been proposed in [10]). A numerical solution of the Frankel equation can be found in [11], and in [12] an interesting study of the behavior of laminar flames with a very large radius. We shall be concerned here with the problem of turbulent flame fronts submitted to the Darrieus-Landau instability; a variant of the Frankel equation, coupled to a treatment of reconnections occurring on the front, will be used for this purpose.

Let us first recall the usual form of the Frankel equation. Let us note by **n** the local normal vector at a given point of the flame, which is assumed to have the topology of a closed contour. **n** will be chosen to point in the direction of flame propagation. The evolution of the front is completely described by specifying the normal velocity of the flame at each point of the contour. This normal velocity is the sum of two terms: a first term $u_1(1-\varepsilon\kappa)$ represents the flame velocity: it is given by the laminar velocity u_1 corrected by a term proportional to the curvature κ (ε being a constant usually called the Markstein length). The values $u_1=1$ and $\varepsilon=0.1$ will be used in the simulations presented in this paper. A second term corresponding to the normal velocity caused by hydrodynamics has to be added to the flame velocity, and the Frankel equation [9] is obtained,

$$V_n(\mathbf{r})=1-\varepsilon\kappa-\alpha\left[1-\frac{1}{\pi}\int\frac{(\mathbf{r}-\xi)\cdot\mathbf{n}}{|\mathbf{r}-\xi|^2}dl_\xi\right], \qquad (1)$$

where the integration is taken over the contour, and α is a parameter controlling the importance of the hydrodynamic instability. In the case of a circle and $\varepsilon=0$, the normal velocity V_n becomes simply 1, as has been shown in the original article of Frankel [9]. If we consider the growth rate $\sigma(k)$ of sinusoidal perturbations with wave vector k applied to a plane flame, $\sigma(k)$ has the form

$$\sigma(k)=\alpha|k|-\varepsilon k^2, \qquad (2)$$

where α and ε are the coefficient appearing in Eq. (1).

Note that Eq. (1) is derived in the case where the flow is potential, this potential being created by the contour uniformly charged with charge α/π. If we define the temperature of unburnt gases by T_u, the temperature of burnt gases by T_b, and by γ the gas expansion parameter $\gamma=(T_b-T_u)/T_b$ it can be shown [9] that $\alpha=\gamma/2$, when γ is small if the unit of length is the flame thickness and the unit of time the transit time through the flame. However, although the Frankel equation and the Michelson-Sivashinsky equations are derived rigorously only when γ is small, it has been found [4] that the real domain of applicability of these equations is much wider if α is simply chosen as the slope at the origin of the dispersion relation (2), for a finite γ, and if ε is chosen to give the good domain of unstable wave vectors.

Let us now consider the problem of turbulent flames with gas expansion. In principle, it would be sufficient to add to the normal velocity of markers defined by the Frankel equation [Eq. (1)] the turbulent velocity of the flow without flame. Such an approach has been used in [5] in the case of the Michelson-Sivashinsky equation. Then the markers would evolve according to the total velocity.

However, the two-dimensional problem is not so simple. When a turbulent velocity field is taken into account, reconnections occur on the front, forming new pockets which separate from the original one. We must have a way to describe the different pockets, and to perform the reconnections.

Concerning the first problem, the Frankel equation can be extended to the case where the front consists of a finite number of pockets, each with its own propagation direction (burnt gases surrounded by fresh gases or fresh gases surrounded by burnt gases). As the potential leading to the velocity in Eq. (1) is simply an electrostatic potential of a line uniformly charged, we can add the potentials of all the pockets because of a superposition principle, and we obtain

$$V_n(\mathbf{r}) = 1 - \varepsilon\kappa - \alpha\left(1 - \frac{1}{\pi}\sum_P \int_P \frac{(\mathbf{r}-\xi)\cdot\mathbf{n}}{|\mathbf{r}-\xi|^2} dl_\xi\right), \quad (3)$$

where we have added a sum over all pockets, and each integral is taken over one pocket P (the integrals are simply computed by a trapezoidal rule). The displacement of a point at position $\mathbf{r}$ being given by

$$\frac{d\mathbf{r}}{dt} = V_n(\mathbf{r})\mathbf{n} + \mathbf{V}(\mathbf{r},t), \quad (4)$$

where $\mathbf{V}$ is the turbulent velocity field.

Now, we come to the reconnections problem. A way to handle this problem with a Lagrangian method has been indicated in [13] for the case of a front at zero heat release. We give here a summary of the method used, which can be decomposed into different stages. At each time step, the front is first submitted to a propagation stage [Eq. (4)]. As a result of this propagation (and of the turbulent velocity field) the front can present self-intersections. These intersections indicate that a reconnection is occurring. In the second stage the intersections are detected, and the third stage consists in performing the reconnection detected. Finally, in the fourth stage, the mesh points on the front are adapted.

We have described, for the moment, how the propagation state can incorporate a nonzero heat release through the use of the Frankel equation. Let us describe the intersections detection stage. We do not examine if each couple of segments intersect each other. It would be a waste of computer time, as segments in most couples are relatively far from each other, and have no chance to intersect. So we divide the domain in several boxes, a segment belongs to a box if it crosses this box, and we only look for intersections inside each box. Once the intersections are detected, we perform the reconnection associated to the intersection pattern, if it is recognized by the program. An example of a rule implemented is shown in Fig. 1. This type of reconnection causes the creation of a new pocket. If the reconnection is not recognized by the program, we take the solution at the previous time and reduce the time step until the reconnection is recognized. Once the reconnections have been performed, we adapt the mesh by inserting new points where the mesh size is too great or deleting points where points are too close. During the adaptation process, we also delete pockets of fresh gases which are too small.

We choose the following turbulent field (V, V_y):

$$V_x = -\sum_{k_i} a k_i^{-5/6} \cos(k_i x + \varphi_{ix}) \sin(k_i y + \varphi_{iy}) \cos(\omega_i t), \quad (5)$$

$$V_y = \sum_{k_i} a k_i^{-5/6} \sin(k_i x + \varphi_{ix}) \cos(k_i y + \varphi_{iy}) \cos(\omega_i t), \quad (6)$$

where a controls the amplitude of the turbulent field. The possible wave vectors in the computational domain are $k_i = (2\pi i)/30$, where i is an integer number ranging from 5 to 100. φ_{ix} and φ_{iy} are constant random phases associated with the wave vector k_i. All the simulations presented correspond

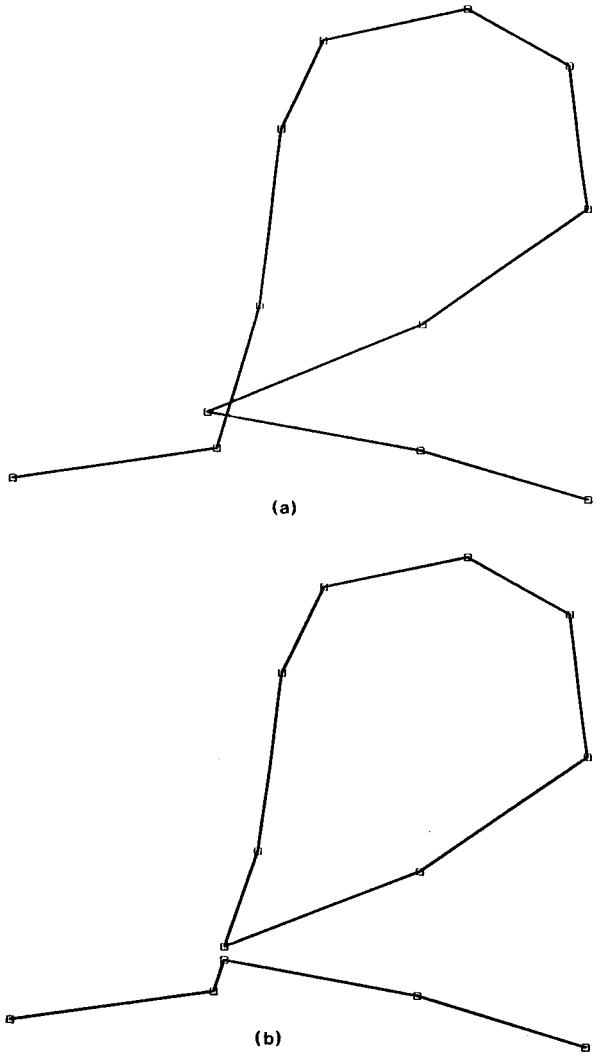

FIG. 1. Reconnection of a self-intersecting front. (a) The front before reconnection. (b) The front after reconnection: a pocket has been created, a point has been deleted, and two new points corresponding to the two intersections have been created.

to the high value $a = 12$ for the amplitude. The turbulent intensity u' corresponding to the value of a can be calculated by the Parseval equality

$$u' = \left[\frac{1}{4}\sum_{k_i} (a k_i^{-5/6})^2\right]^{1/2}. \quad (7)$$

We obtain for $a = 12$ the value $u' = 15.3$ which is very high compared to the laminar velocity, which is 1 here.

The velocity field is incompressible and contains several different scales. The amplitude at a given scale $(a k_i^{-5/6})$ corresponds to a Kolmogorov spectrum [i.e., $a k_i^{-5/3}$ spectrum for $E(k)$] for this anisotropic flow field. This spectrum decreases more quickly as k increases than the spectrum taken in [13].

Another difference with this paper is that here we do not select a frozen flow field and take into account time decorrelations through the term $\cos(\omega_i t)$. We will perform calculations corresponding to the two values $\omega_i = 3 a k_i^{1/6}$ and

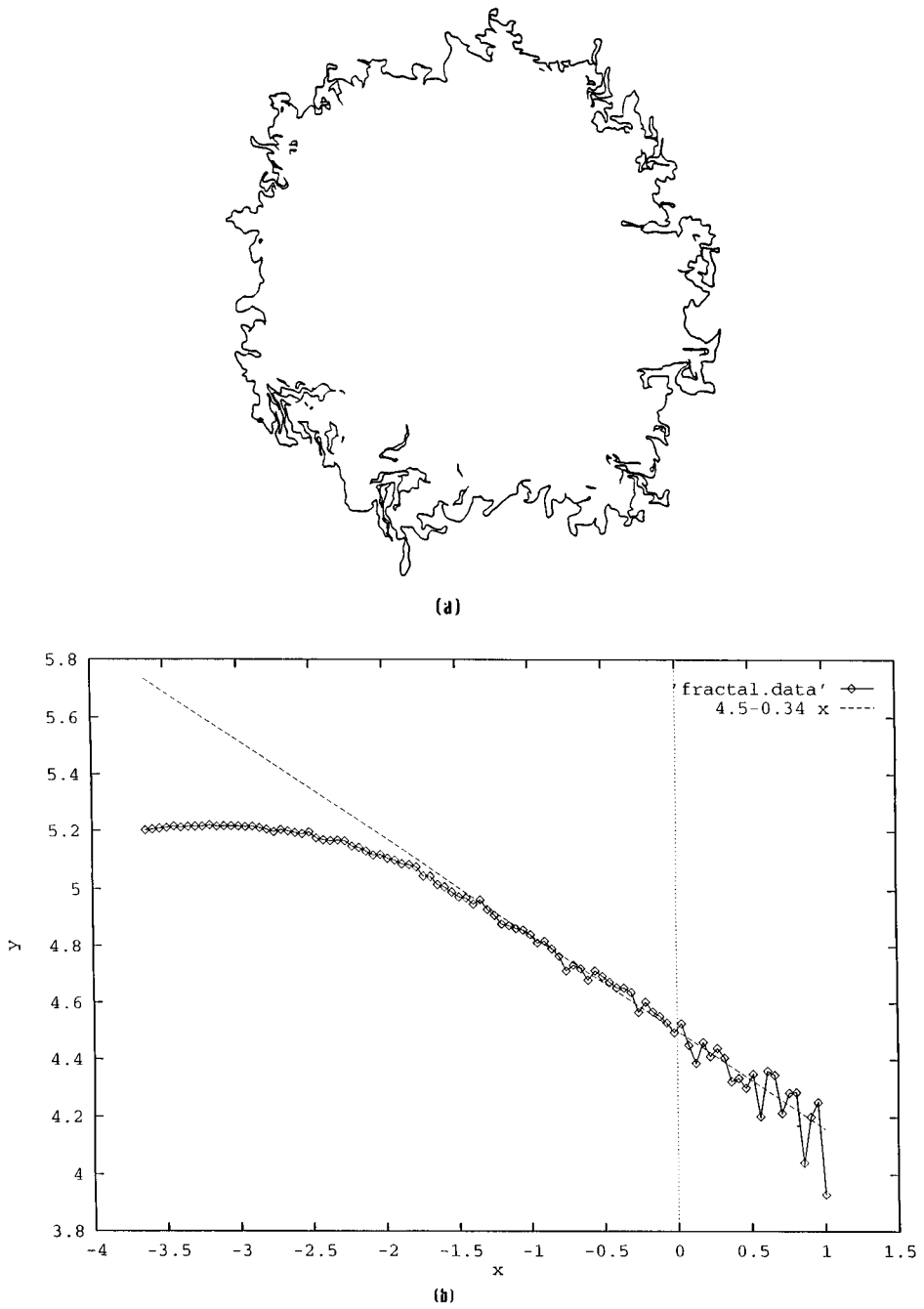

FIG. 2. (a) Propagating front for $\omega_i = 3ak_i^{1/6}$ and $\alpha = 0$ (the front is propagating outwards). (b) Plot of $\ln(S)$ vs $\ln(dx)$ for the previous front.

$\omega_i = 3ak_i^{2/3}$ in order to have an idea of the effect of decorrelations on the fractal dimension. Let us note, however, that the front propagates through the turbulent field, and generates its own decorrelations because of the propagation. Depending on parameters, the decorrelation due to propagation could be dominant (i.e., correlation times smaller) compared to decorrelation due to turbulence itself over a range of scales.

We start with a pocket of burnt gases surrounded by fresh gases of radius 5, and let it evolve until it presents a fractal form with a fractal dimension approximately constant in time. The time that we have to wait is relatively short, approximately 0.5, which can be compared to a maximum growth rate 0.4 (typical growth time of instability 2.5) when $\alpha = 0.4$ (in time units corresponding to $\varepsilon = 0.1$). This time can also be compared to the larger correlation time (at large scale) of the turbulent field which is approximately 0.2 in our simulations.

We define the fractal dimension of the front by a box counting method: we cover the domain with squares of size dx and see how many boxes N are occupied by a portion of the main pocket. We obtain a length $S = N^* dx$ of the main pocket, and plot $\ln(S)$ measured at this scale, versus the logarithm of the scale $\ln(dx)$. The fractal dimension d_f is one minus the slope of this curve. We consider the fractal dimension of only the main pocket and not of the main and secondary pockets, because for large turbulence intensities, very small pockets are created, which are not at all fractal and should not be included in the box counting. Contrary to [13], we use here a fractal dimension given by a box counting method and not by comparing the lengths of polygonal approximations of the front at different scales, because we

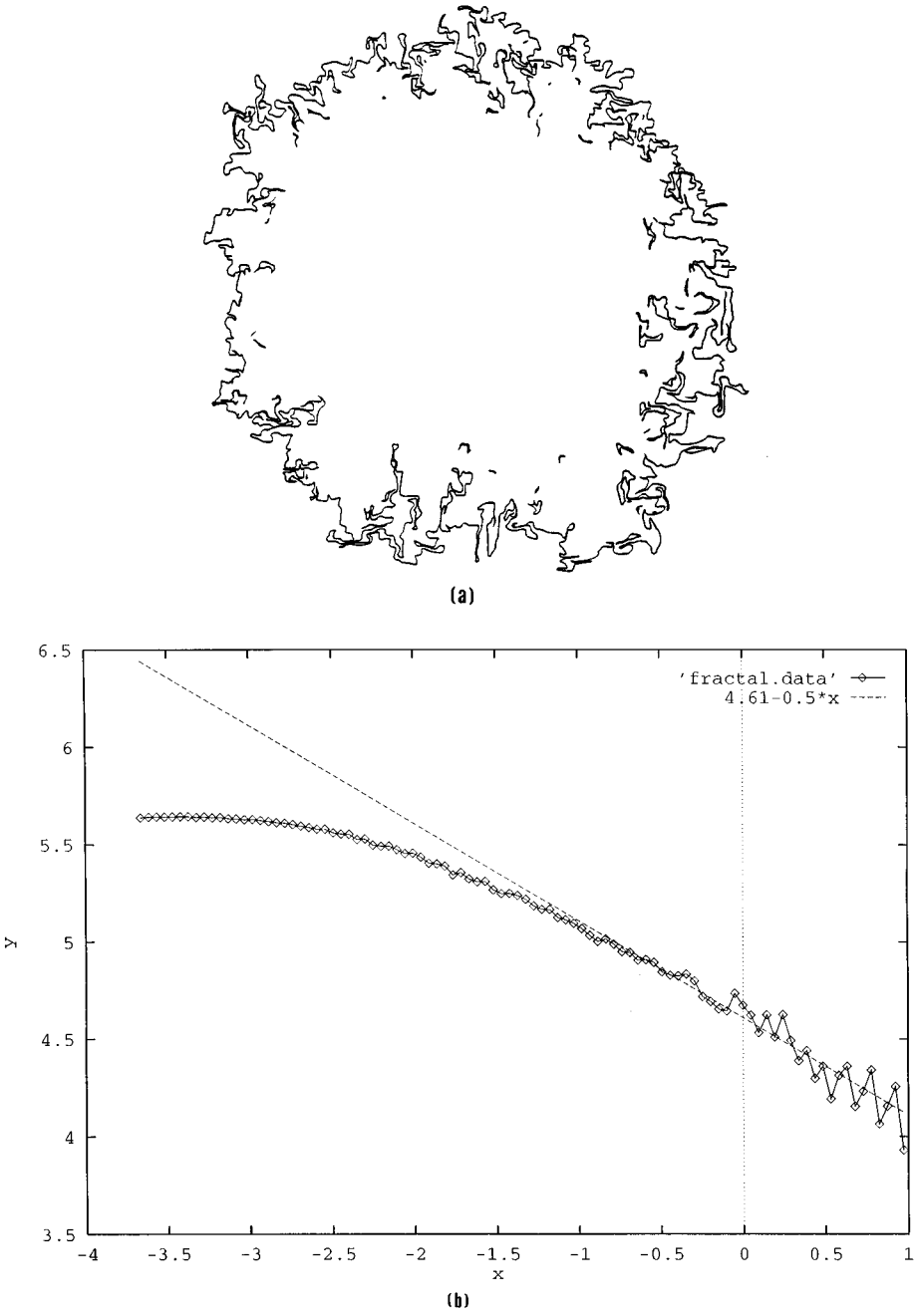

FIG. 3. (a) Propagating front for $\omega_i = 3ak_i^{1/6}$ and $\alpha = 0.35$. (b) Plot of $\ln(S)$ vs $\ln(dx)$ for the previous front.

have found that for high values of heat release, the polygonal fractal dimension is noticeably higher than the box counting fractal dimension and seems less reliable.

In Fig. 2(a), we show in the case $\omega_i = 3ak_i^{1/6}$a front obtained for $\alpha = 0$ (zero heat release). The front has a fractal dimension $d_f = 1.34$, as seen by the slope of the curve $\ln(S)$ vs $\ln(dx)$ in Fig. 2(b). In Fig. 3(a), we take (for the same value of ω_i) $\alpha = 0.35$: we obtain a fractal dimension $d_f = 1.50$. The curve $\ln(S)$ vs $\ln(dx)$ is given for this case in Fig. 3(b). Because of the variation in time of the fractal dimension measured and of the choice of the line giving the slope of the curve, the fractal dimensions obtained are not very precise and we expect a typical error of the order of ± 0.02.

We now examine the case $\omega_i = 3ak_i^{2/3}$, which corresponds to the scaling of decorrelations expected for Kolmogorov turbulence. Compared to the previous case (Figs. 2 and 3), where the correlation time was slowly varying, the correlation time is approximately the same at large scales, but is much lower at small scales. In this case, the measurement of the fractal dimension is more difficult and we estimate a typical error to be ± 0.03. In Fig. 4, a front obtained for $\alpha = 0$ is shown, with a fractal dimension $d_f = 1.33$, very close to the value of Fig. 2(a). In Fig. 5, we have $\alpha = 0.4$: the fractal dimension is now $d_f = 1.46$.

The dependence of the fractal dimension with α is shown in Fig. 6 for both values of correlation time. Because of the errors involved in the measurement of the fractal dimension, the points are relatively scattered, and we also give in this figure a fit for each value of the correlation time. For low values of α the two curves are relatively close, giving a fractal dimension close to 1.34; however, when α increases,

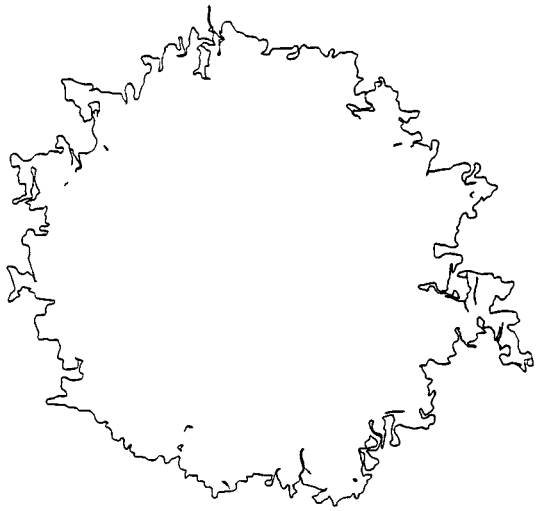

FIG. 4. Propagating front for $\omega_i=3ak_i^{2/3}$ and $\alpha=0$.

the curve corresponding to $\omega_i=3ak_i^{1/6}$ (i.e., larger correlation time) is higher and seems to saturate for high values of α, i.e., very exothermic flames, corresponding to typical fronts, as seen in Fig. 3(a). On the contrary, the curve corresponding to $\omega_i=3ak_i^{2/3}$ increases in a much slower way, Fig. 5 corresponding to the last point of this curve. We recall that this scaling of ω_i corresponds to the one in Kolmogorov turbulence.

It is important to have an estimate of the value of α corresponding to a typical flame encountered in experiments, in order to locate this typical point on Fig. 6. We consider a flame with $\gamma=0.8$, corresponding to burnt gases with a temperature five times higher than the temperature of fresh gases. It has been difficult to measure Markstein lengths experimentally, but it seems typical values of this parameter range from 4 to 8 [14,15] (in units of flame thickness). The value of α in units deduced from the flame thickness and the transit time is, as explained before, obtained by considering the first term of the development of the dispersion relation with k, and gives the value, already obtained by Landau [16]

$$\alpha=\frac{1}{2-\gamma}\left(\left[\frac{1+\gamma-\gamma^2}{1-\gamma}\right]^{1/2}-1\right). \tag{8}$$

Now we have to normalize α with the units used in this paper, i.e., corresponding to $\varepsilon=0.1$. If we take a Markstein length of 4, we obtain $\alpha=0.16$. A Markstein length of 8 would give an even lower value $\alpha=0.11$. It is easily seen in Fig. 6 that these values of α correspond on the lower curve (Kolmogorov temporal scaling) to a relatively small increase in fractal dimension due to gas expansion. Thus we can justify to a large extent the usual approximation of zero heat release used in many theoretical and numerical works on turbulent premixed flames (see [1], for instance). Even for $\alpha=0.16$ and on the higher curve, i.e., for a maximum value of the fractal dimension, we only obtain an increase of approximately 0.1 compared to the value at zero heat release. For the typical values of α, the value we get (on the lower curve) for d_f for this particular flow field is comparable to values usually obtained in experiments for high amplitudes of forcing. We recall here for purpose of comparison the value $d_f=1.38$ obtained in [17] in a propane engine.

This increase in fractal dimension caused by heat release is measurable in experiments by varying the equivalence ratio while fixing the ratio of the amplitude of forcing to the laminar flame velocity. In general, the variation of the Markstein length with the equivalence ratio has to be taken into account, and this complicates the interpretation of the experimental results, as the Markstein length is difficult to measure experimentally. The result suggested by this paper that the effect of heat release is relatively small for typical flames seems to be compatible with experiments (see, for instance [18]), which describe the fractal dimension as a function of the ratio of amplitude of forcing to laminar velocity, without taking into account at all the effect of heat release. However, this effect should not be small in the case of a very exothermic flame with a low Markstein length, which gives a more important value of α in Fig. 6.

In this paper, by using a modified version of the Frankel equation in combination with a treatment of reconnections occurring during propagation, we have been able to simulate turbulent premixed flames submitted to the hydrodynamic

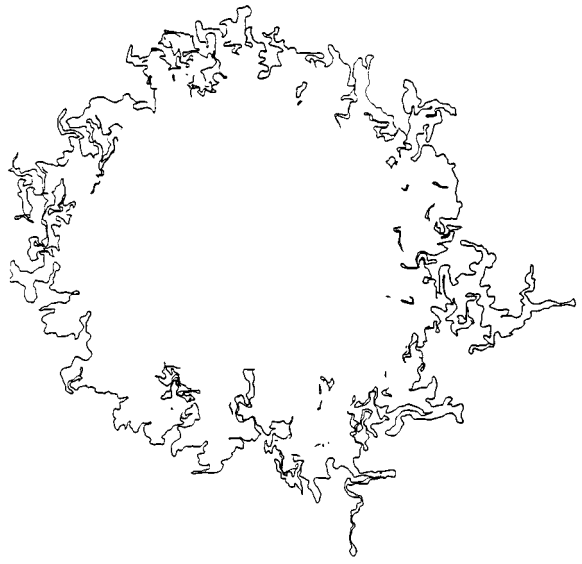

FIG. 5. Propagating front for $\omega_i=3ak_i^{2/3}$ and $\alpha=0.4$.

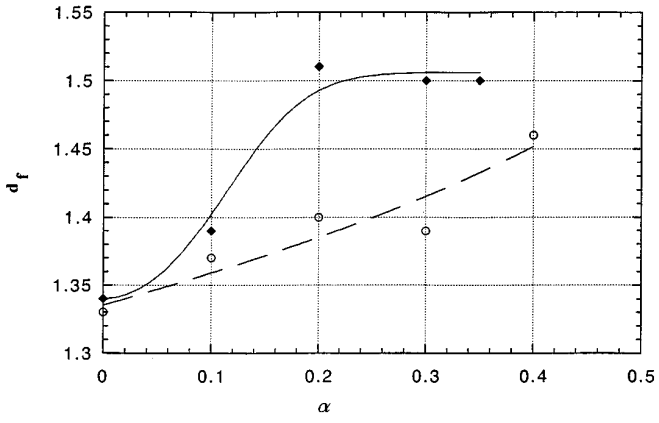

FIG. 6. Fractal dimension d_f vs α: numerical results for $\omega_i=3ak_i^{1/6}$ (black diamonds), for $\omega_i=3ak_i^{2/3}$(white circles), fit for $\omega_i=3ak_i^{1/6}$ (solid line), fit for $\omega_i=3ak_i^{2/3}$(dotted line).

Darrieus-Landau instability. This work suggests that for typical values of gas expansion, the increase of fractal dimension with heat release is relatively low. This study is performed with a simple model of turbulent field, but others, more realistic turbulent fields could be used in the framework provided in this paper. A comparison with experimental works (in a three-dimensional configuration, with realistic turbulence) should however be done before a definitive conclusion on the effect of heat release is obtained. In any event, heat release is important for low and moderate forcings. The Frankel equation used in this article could be very useful in case of moderate forcings, where the front position cannot be described by a function of the angular coordinate, and a truly coordinate-free formulating is necessary.

[1] A. R. Kerstein, W. T. Ashurst, and F. A. Williams, Phys. Rev. A **37**, 2728 (1988).
[2] G. I. Sivashinsky, Acta Astron. **4**, 1117 (1977).
[3] D. M. Michelson and G. I. Sivashinsky, Combust. Flame **48**, 211 (1982).
[4] G. Joulin and P. Cambray, Combust. Sci. Tech. **81**, 243 (1992).
[5] P. Cambray and G. Joulin, in *Twenty-fourth Symposium (International) on Combustion* (The Combustion Institute, Pittsburgh, 1992), p. 61.
[6] B. Denet and J. L. Bonino, Combust. Sci. Tech. **99**, 235 (1994).
[7] L. Filyand, G. I. Sivashinsky, and M. L. Frankel, Physica D **72**, 110 (1994).
[8] P. Cambray, K. Joulain, and G. Joulin, Combust. Sci. Tech. **112**, 271 (1996).
[9] M. L. Frankel, Phys. Fluids A **2**, 1879 (1990).
[10] W. T. Ashurst, Combust. Sci. Tech. **109**, 227 (1995).
[11] M. L. Frankel and G. I. Sivashinsky, Phys. Rev. E **52**, 6154 (1995).
[12] S. I. Blinnikov and P. V. Sasorov, Phys. Rev. E **53**, 4827 (1996).
[13] B. Denet, Combust. Sci. Tech. **123**, 24 (1997).
[14] G. Searby and J. Quinard, Combust. Flame **82**, 298 (1990).
[15] B. Deshaies and P. Cambray, Combust Flame **82**, 361 (1990).
[16] L. Landau, Acta Physicochim. URSS **19**, 77 (1944).
[17] J. Mantzaras, P. G. Felton, and F. V. Bracco, Combust. Flame **77**, 295 (1989).
[18] A. Yoshida *et al.*, Combust. Sci. Tech. **103**, 207 (1994).